ISSN 0074-655X

Bulletin of the International Institute of Seismology and Earthquake Engineering

Special Edition

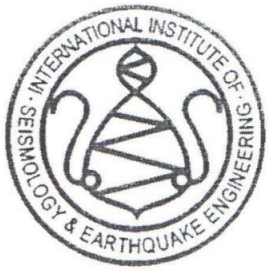

BUILDING RESEARCH INSTITUTE

2003

SEISMIC HAZARD ASSESSMENT OF WESTERN SAUDI ARABIA AND THE RED SEA REGION

by

A.M. Al-Amri B.T. Punsalan A. R. Khalil E. A. Uy

ABSTRACT

A preliminary seismic hazard assessment of western Saudi Arabia is represented in two single element maps. These are the expected maximum intensity and ground acceleration in 100 years at 10% probability of exceedance. Three sub-areas of seismic concern were identified and delineated. These are the land and coastal areas covered by the range of intensities from VI-VIII. This preliminary assessment can be considered as conservative estimate and supplemental information about earthquake hazards in the region.

INTRODUCTION

The western part of Saudi Arabia is composed of the Red Sea and the shield. The Red Sea is a region of international interest, for observation and study of rifting and subsequently drifting continents. It has a young diverging mid-oceanic ridge. The Red Sea is approximately 2200 km long and may be classified into three physiographic regions. These are the continental margins, the main trough, and the deep axial trough [1]. High heat flow emanates from the axial trough. Deep holes are observed to be present in the mid-ridge. However, both these observed geophysical phenomena are not uniformly distributed. Intense crustal deformation is taking place in the mid-ridge, but with scattered concentration of spatio-temporal seismic activities (fig. 2). The axial trough is a source of seismic events as well as the NE trending transform faults located by geophysical studies [2,3]. The faults are distributed along the Red Sea profile with probable extensions toward inland on both sides (figs. 1-2). Another prominent seismic source is the NE trending southern Dead Sea transform fault that is approximately 1100 km long passes through the gulf of Aqabah. This fault has been historically active [4,5]. Supplemental to the transform faults are the numerous NS, NW, and NE trending land faults and lineaments in the western portion of the Arabian shield. These faults and lineaments are not considered seismically active at present in terms of moderate to strong earthquake events, but may be seismogenically related to existing major fault systems in the area. In north Yemen is the Sadah fault and its volcanic terrain known as the Yellow Trap Series. On the western margin of the Red Sea, other rift systems are present, transform faults, and volcanic ranges that have been seismically active in the past [5]. These are the Afar and western extension of the Aden rift systems, the Danakil transform fault, and volcanic ranges in Afar. These seismogenic zones are sources of earthquake hazards in the respective region where the source areas are located.

The space-time distribution of seismic events in western Saudi Arabia suggests that the active transform and land faults, the southern and northern portions of the Red Sea rift systems, and volcanic ranges are the

sources of earthquake hazards in this area. It is imperative that earthquake hazards from these sources be assessed, for the minimization and mitigation of earthquake losses, and for the implementation of planning and socio-economic development.

The study area encompasses the Red Sea from latitude 12N to 30N degree north, and the land areas covered by approximately a perpendicular distance of 4 degrees from the axial trough toward inland on both sides, forming a rectangular shape whose axis length is parallel to the Red Sea and with a width of 8 degrees. The outline and shape of the study area is not strictly fixed but depends upon the availability of seismic data. Figs. 1 and 2 are the maps of tectonics and seismicity respectively in the study region.

Different methods of approach and distribution equations have been developed and applied in evaluation of seismic hazard, e.g. Kawasumi [6], Cornell [7], Algermissen et al [8], Hattori [9], Schenkova et al [10], Boore and Joyner [11], Kijko and Sellevol [12], and the applications of Poisson distribution and Gumbel's [13] theory of extremes. The methods usually take into account the source-propagation-site effects using the free or arbitrary zone method to obtain a frequency law of earthquakes for the seismic parameters of interest at arbitrary points. From the frequency relation, the seismic hazard or expected maximum value of ground motion for a given interval of time is then estimated using probability distribution.

Some of these methods have been applied in some related studies of western Saudi Arabia and adjacent areas [14,15,16,17,18,19,20] based on arbitrary zonation of the seismic sources. The knowledge and lessons obtained in their respective study areas are enlightening and informative. However, appropriateness of the applied attenuation models to local conditions may require further comparative study. Another alternative approach, proposed here is thought to give more realistic results for supplemental source of seismic hazard information in the area of interest. This approach is the utilization of the free zone method, empirically determined intensity attenuation equation and other related relations from local data. The application of the free zone technique [6] and the empirical relations provide another process of integrating ground motion effects at arbitrary points in the study area for statistical analysis.

The free zone method is safer to use and deemed more appropriate from the physical point of view, for what are considered are the actual and observed seismic events [6], although randomness of earthquake occurrences in space-time is a reasonable assumption. However, non-uniform occurrence of seismic events is an observed phenomenon even in seemingly considerable one geological unit [21]. It is a matter of interest to consider this observation in seismic hazard assessment in the region. A study of seismic hazard assessment is then undertaken based on this alternative for western Saudi Arabia, within the limitations of the available seismological data as initial hypothesis.

Data Sources and Reliability

Four main sources of seismic data are merged for utilization in the study. These are the seismic data files from the United States Geological Survey (USGS/NEIC), the International Seismological Center (ISC), the Seismic Studies Center (SSC) of King Saud University, and the European Mediterranean Seismological Center (EMSC). Other source of data comes from Amraseys [5] compilation of seismic events for Saudi Arabia and adjacent areas.

Generally, the USGS and ISC data cover the period from 112 – 2000. Missing historical events prior to 1900 from the USGS and ISC files are augmented and referred from Ambraseys [5] compilation. The latter period from 1986 onward is taken mostly from the SSC and EMSC bulletins for magnitude less than 5. In 1985, the SSC of KSU (formerly Seismological-Geophysical Observatory) was established. The Center has installed initially 22 seismic stations in the eastern portion of the Red Sea and central part of Saudi Arabia. The operation of the stations paved the way for comprehensive monitoring of seismic events in the area for reliable database.

Because of the unavailability of local acceleration data suitable for attenuation study, the parameter intensity is used as a measure of seismic assessment. For comparative analysis to other works, the expected maximum intensity is converted to ground acceleration using empirically developed conversion equation. Intensity does not fully satisfy designer's requirements. However, its simplicity and complexity, and the necessity of re-evaluation of historical records as database for long pattern of seismicity makes its application essential in investigation [24]. The present utilization of this parameter to seismic hazard assessment in the region may provide useful information, and may serve an impetus and a tool for further undertakings within the premise of investigating seismicity pattern.

The very small number of seismic monitoring stations in the study region in the early part of the previous century certainly affects the completeness and the accuracy in the locations and magnitudes of the earthquake events in the study area. It was only in 1965 that the magnitude and location determination of seismic events have considerably improved due to the establishment and operation of the World Wide Standardized Seismograph Network (WWSSN) of the USGS. Magnitudes of earthquakes in the USGS and ISC seismic bulletins were mostly calculated for the body waves. The bulk of seismic data starts in 1965 and this contributed significantly to the study. The body-wave magnitude (mb) was preferably used in the study due to this fact and the relative consistency of data using this type of magnitude for values equal and less than 6.5. Notably, most observed magnitudes in the region are below 6.5, and only few are above this value. It is also assumed that the calibration of duration and local magnitude formulas developed in the area are based on the mb as the standard statistical value. Hence, for values of duration and local magnitudes from 3.5 and above are assumed to be equal to mb when magnitude values of 5.0 and above are not available from USGS, ISC or EMSC seismic bulletins.

To improve the seismic data for the study, efforts are conducted in performing relocation of epicenters, conversion of the different types of magnitudes which are the surface and macroseismic to body wave type, and verification of doubtful entries. The re-calculations of the SSC locations in NW Saudi Arabia make use of the additional phase readings provided by EMSC. These were furnished when the Joint Seismological Observation Period (JSOP) experiment was conducted in 1994 to 1996, in an area defined by coordinates: 24-35N ; 30-40E. The results of re-computations indicate an average distance discrepancy of 20 km from 15 events using the HYPO 71 [25] software and the Jordanian Seismological Observatory (JSO) velocity model. The discrepancy is significantly small to affect ground motion values obtained from the applied attenuation model for the previous and relocated epicenters. In view of the standard error of estimates obtained from the conversion relation for magnitude and intensity, the bounds for magnitude and intensity are 0.5 and one degree respectively, while 20 km for location. Reliability of magnitude, intensity, and location within these values are also recognised by other authors [22,,26,27].

METHOD OF ANALYSIS

The general outline of the methods of analysis are as follows: (1) application of the free zone method in the estimation of ground motion effects at different sites using an appropriate intensity attenuation model; and (2) expectation of the maximum ground motion effects estimated from the intensity-frequency distributions at sites for some interval of time utilizing Poisson process.

(1)Estimation of ground motion effects

The parameter used in seismic hazard assessment of western Saudi Arabia is the seismic intensity in the Medvedev-Sponheuer-Karnik (MSK) [28] intensity scale. To obtain the required intensity data in each site of interest, the study area was subdivided into grid points which are located at every half degree (0.5) latitudes and longitudes. The grid points are the sites at which intensity induced by surrounding seismic events are calculated from the following empirical intensity attenuation equation and other conversion relations:

$$I = Io - 2.2\log(D+6) - 0.015D + 1.7 \quad (1)$$

$$Ms = 0.65Io + 0.9 \quad (2)$$

$$Ms = 1.07mb - 0.476 \quad (3)$$

and

$$CosD = SinXeSinXi + CosXeCosXiCos(Ye-Yi) \quad (4)$$

where I is the intensity at epicentral distance (D), Io is the intensity at the epicenter, X is latitude and Y is longitude. The subscript i refers to the sites and e represents epicenters of seismic events. Ms and mb are the surface-wave and body-wave magnitude respectively.

Equation (1) was the result obtained from isoseismal maps of 10 strong earthquakes from the region. Mean epicentral distance of respective intensity in each map were estimated from sufficiently drawn diagonal lines from the epicenter. Then plot of the intensities with respective distances are drawn for each event. The graphs from the plots are fitted with the equation I=Io-klogD-mD using regression analysis to determine the constants k and m. From the initial findings which are composed of ten (10) k and m values, the final outcome which is equation (1) is the result of generating representative values for the k and m from the initial 10 values. The approach and procedure for obtaining equations (1 and 2) are described in the paper of Punsalan and Al-Amri [29]. Equations (1 and 2) are as shown in figs. (3 and 4), while relation (3) is taken from Al-Amri [30].

Eliminating Ms and Io in relations (1), (2) and (3), equation (1) can be re-written as

$$I = 1.64mb - 2.2Log(D+6) - 0.015D - 0.4 \quad (5)$$

Equations (4) and (5) when combined yield a relation for I in terms of magnitude and coordinates of an event. This relation is used in the estimation of ground motion in the study region. I in each intensity class Ii is $Ii-0.4<I<Ii+0.5$.

(1a) Intensity-frequency relation

The determination of the respective intensity-frequency relation at each site is composed of two steps. The first step is to make a plot of the frequency [n(Ii)] against respective intensity class (Ii) (fig. 5). The second step is to select the best fit equation for the plotted values and employing regression techniques for the determination of the required constants. It is observed that most of the plots indicate logarithmic trend. Others have appropriate data points that fit well the logarithmic trend, while there are plots whose data points are above and below the trend. Further, there are plots with no data in some Ii class. Data points above the trend could be due to the influence of foreshocks, aftershocks and swarm types of earthquake events [26, 33], or superposition of neighboring source areas. Plots with no data points in some higher intensity class could probably be due to moderate seismicity or an incomplete period of observation of earthquakes generating this level of intensity. These phenomena are presumably difficult to separate from the normal seismic activity. Likewise, there is no known rule to us regarding definite method of eliminating the effects of these phenomena in the compiled intensity data. To at least reduce the errors from unequal distribution of the frequency of intensity classes, the cumulative number [N(Ii)] was preferably utilized. Since, the logarithmic trend is mostly observed among plots, the linear relation

$$\log N(Ii) = aIi + b \qquad (6)$$

is fitted in each plot. Minimum number of data points in each plot is 4 when possible. Some of the [log(N(Ii), Ii] plots are shown in figs. (6-7). Fitting of equation (6) may represent an average distribution function as a result of superposition of the different types of earthquake events and seismic activity in the area. To minimize the influence of the superposition as required by the independency of seismic events, a rough way of elimination has been conducted in this paper. From the plots, eye-fitted straight lines are tentatively drawn. The logN(Ii) which are relatively way-off the line relative to the higher intensity classes are assumed to be either due to the presence of foreshocks or aftershocks or swarm activities. The higher intensity values are presumed to be caused by seismic events instrumentally recorded widely in the region and are therefore relatively determined accurately. The way-off values are reduced accordingly in proportion to the reliable data points. The mean rate in equation (6) is obtained by dividing it with the period of observation, T,

$$N(Ii)/T = (1/T)\exp(AIi + B) \qquad (7)$$

where A= aln(10) and B=bln(10).

(2) Expectation of maximum effects estimated from the frequency relations at sites utilizing Poisson process.

(2a) Expected maximum intensity

The cumulative probability p(I) of events equal and larger than a value of interest (I) at each site is [6]

$$p(I)= N(I)/N \qquad (8)$$

where N is the total number of events. Assuming that ground motion occurrences in the study area satisfy the Poisson process, the occurrence probability of p(I) in time t is [24]

$$Pn(I)= (p(I)ht)^n*\exp(-p(I)ht)/n! \qquad (9)$$

where Pn(I) is the probability of occurrence of I in time t, n is the number of event I, and h is the mean rate of occurrence during t. The probability of occurring or exceeding I in time t is [24]

$$Po(I)= 1-\exp(-p(I)ht) \qquad (10)$$

Of importance in seismic hazard estimates is the expected maximum Im during t, given a fixed probability of occurrence Po(I). From (7), (8), and (10), the value of Im in each site can be estimated which is

$$Im = -B/A + (1/A)\ln(-(T/t)\ln(1-Po(I)) \qquad (11)$$

Hence, for seismic hazard estimates in the study region, (11) is applied for values of Po(I)= 10% and t= 100 years. These values were selected in consideration to lifetime of building structures and to the level of seismicity in the area. The calculated values are plotted at respective sites as bases for contouring the iso-curves.

(2b) Iso-acceleration curves

The calculated values in (11) are converted to peak ground acceleration using

$$\log A = 0.3I - 0.014 \qquad (12)$$

from Trifunac and Brady [36], where A is the horizontal acceleration in gals (cm/sec-sec). The A values are expressed in percent of the acceleration of gravity (g), plotted and contoured for supplemental information about seismic hazard in the region as well as for comparative analysis.

DISCUSSION & CONCLUSION

The results are shown in figs. (8-9). The highest expected maximum intensity at 10% probability of exceedance in 100 years is VIII. These are located approximately in the area of (20N, 39E) and (14N, 44E). Essentially, the main seismic concern is the coastal and land areas covered by the range of intensities from VI to VIII, allowing ground motion dependence to medium properties. This range of intensity can caused slight to heavy damage to many reinforced structures and wooden houses; from moderate to total collapse of many pre-fabricated and half-timbered structures; and from heavy to total collapse of adobe and clay houses, as defined by the MSK scale.

The range of intensity values from VI-VIII may be subdivided into three sub-areas. These are the northern part (top) from 26N to 30N, the western and eastern flanks of the southern Red Sea from 12N to 22N, and the southern part of Saudi Arabia including Yemen from 12N to 16N. The approximate latitudes of separation are at 23 and 14 degrees north. In the top sub-area, the approximate coastal and land area covered by the intensity range VI-VII is from latitude 25 to 30 degrees north. This sub-area is prone to destructive earthquakes since historical time (fig. 2). The sub-area includes places and cities such as Haql, Ouyannah, Bada, Makna, Tabuk, Dubai, and Wajh. The middle and bottom sub-areas are from latitude 12 to 23 degrees north, covering some portions in the Asir region and Yemen in the western side of the Arabian shield, and the countries Ethiopia, Eritria, and parts of Sudan in the western flank of the Red Sea. Some places and cities covered by this range are Jeddah, Taif, Abha, and Jizan in western Saudi Arabia, Dhamar and Sana in Yemen.

Fig. 9 is the converted values obtained in equation (11) to ground acceleration using (12). The iso-acceleration curves of the present study moderately differ in ground acceleration values, shape and orientation of contours with the previous studies [18,19,20]. The present method which utilizes free zone technique leads to generation of iso-intensity and iso-acceleration curves that are irregular in shapes. Generally, the contours follow the trend of the space distribution of the seismic activities and to some extent with the known tectonic structures in

the region. Whereas, the zonation method generates contour lines approximately elliptical in shape around the arbitrary seismic source zone covering a wider areas of coverage for the expected largest shocks. Within the active areas of seismic activities, both present and past studies are agreeable within allowable and reasonable values. Al-Haddad et al [19] obtained from 0.3g-0.2g for the gulf of Aqaba and its coastal areas and for Jizan, and from 0.15g-0.05g for the other coastal and land areas of western Saudi Arabia; Al-Amri [20] obtained likewise the same values for the southern Red Sea region; Geomatrix [15] is (0.5g-0.1g) for Jizan; and Yucemen and Qa-dan [17] is (0.15g) for the gulf of Aqaba. In fig. 9, the estimated ground acceleration for some places are approximately: 0.05g-0.1g for Abha; 0.05g-0.15g for Tabuk; 0.2g for Haql, Makna, Bada, Ouyannah,: Jizan, Jeddah, and Taif is 0.1g ; for Dubai and Wajh is 0.05g; and 0.2g-0.3g for the gulf of Aqaba.

In the top sub-area, the generating sources of earthquake hazards are the NE trending Dead Sea transform fault that passes through the gulf of Aqaba [31], and the numerous NS, NE, NW trending land faults and lineaments in the Midyan-Hijas region of the western Arabian shield (fig. 1). For the middle sub-area are the NE trending Ad Damm transform fault located approximately at (19.5N, 39E) and its probable extension inland on both side of the Red Sea, the Afar and Red Sea rift systems, and the other transform and land faults [32]. The probable inland incursion of the Ad-Damm fault in the Arabian shield is inferred from magnetic and seismic data [2,37]. In the bottom sub-area, the seismic sources are the Abha syncline located approximately at (17.5N, 42.5E), the NE trending Ad Darb transform fault at about (17N, 41E) and its probable continuation inland, the NW trending Sadah fault located within the vicinity of (15.8N, 44.8E), and the possible extension of the east African rift to Yemen in its volcanic terrain. Furthermore, the common source of earthquake hazards to the three zones is the on-going process of magmatic extrusion along the axial trough of the Red Sea.

A frequent source of uncertainties in seismic hazard assessment are the reliability of seismic data source, dependencies of ground motion on the medium properties, and the large scatter of data in the conversion of one empirical relation to other parametric relation [40]. The scarcity of instrumental data in the study region particularly in the shield areas may yield relatively inaccurate outcomes. This limitation and other constraints such as unreliability of historical data possibly affect the results. Confinement to seismological consideration does not probably reflect the long-term pattern of seismicity. The absence of strong motion network in the area of study constrained the suitable determination of an attenuation model for appropriate application to local conditions. These restrictions affect the validity of the results, thus relegating the obtained values to conservative estimates.

Acknowledgement

Acknowledging and expressing gratitude to Nassir Al-Arifi, Ali Gharib, Hamad Al-Mulhem, and Harun Omar for their valuable assistance in the preparation of the manuscript.

References

[1] Maamoun M, Allam A, Refai E, and Mohamed R J "Neotectonics of eastern Arabian region", Helwan Inst. Astrn. Geophys., Egypt, 1981

[2] Hall S "A total intensity magnetic anomaly map of the Red Sea and its interpretation", Directorate General of Mineral Resources, Jeddah, Saudi Arabia Report 275, 1979, 260p

[3] Makris J and Rihm R "Shear-controlled evolution of the Red Sea pull apart model, Tectonophysics, 198, 1991, 441-466

[4] Ben-Menahem A "Earthquake catalogue for the Middleast (92BC-1980AD), Bull. Geofis. Teor. Appl., 84, 1979,245-310

[5] Ambraseys A "Seismicity of Saudi Arabia and adjacent areas, Report 88/11, ESEE, Imperial Col. Sci. Tech.,London, U.K., 1988

[6] Kawasumi H "Measures of earthquake danger and expectancy of maximum intensity throughout Japan as inferred from the seismic activity in historical times", Bull. Earthq. Res. Inst., 29, 1957, 469

[7] Cornell C A "Engineering seismic risk analysis", Bull. Seism. Soc. Am., 58, 1968, 1583-1606

[8] Algermissen S T and Perkins D "A probabilistics estimate of maximum acceleration in rock in contiguous United States", USGS Open File Report 76, 1976, 416-435

[9] Hattori S "Seismic risk maps in the world (maximum acceleration and maximum particle velocity)", Bull. Inter. Inst. Seism. Earthq. Engg., 17, 1979, 33-96

[10]Schenkova Z, Schenk V, and Karnik V "Seismic hazard estimate for a low seismicity region-example of Bohemia", PAGEOPH, 119, 1981, 1077-1092

[11] Boore M D and Joyner W B "A note on the use of random vibration theory to predict peak amplitudes of transient signals", Bull. Seism. Soc. Am., 74, 1984,2035-2039

[12] Kijko A and Sellevoll M A "Estimation of the earthquake hazard parameters from incomplete data", Natural Hazards, 3, 1990, 1-13

[13] Gumbel E S "Statistics of Extremes", Colombia Univ. Press, 1958

[14] Ali S A "Seismic risk study of Jeddah region in Saudi Arabia", Proc. 18th World Conference on Earthquake Engineering, San Francisco, USA, 1984, 13-60

[15] Geomatrix Consultants "Special geo-technical studies". A report submitted to Ministry of Municipal and Rural Affairs, Deputy of Ministry of Town Planning in Saudi Arabia, Report NJHO, 2, Studies and Investigations, Vol. 3

[16] Al-Noury S I and Ali S A "Seismic risk analysis of western Saudi Arabia", Engg. Geol., 23, 1986, 95-108

[17] Yucceman S and Qa'dan H "Seismic hazard analysis for Jordan", Proc. 2nd Arab Conference on Structural Engineering, Jordan Univ., 1987, 19-22April

[18] Thenhaus P C, Algermissen S T, Perkins D M, Hanson S L, and Diment W H "Probabilistic estimates of the seismic ground-motion hazard in western Saudi Arabia, USGS, Geol. Bull., 1989

[19] Al-Haddad M, Siddiqi G, Al-Zaid R, Arafah A, Necioglu A, and Turkelli N "A basis for evaluation of seismic hazard and design criteria for the Kingdom of Saudi Arabia", Earthq. Spectra 10, 1994, 231-258

[20] Al-Amri A M "Preliminary seismic hazard assessment of southern Red Sea region, Jour. Europ. Earthq. Engg., 3, 1995, 33-38

[21] Ritsema A "Seismology and upper mantle investigation", Geophy. Monogrph., The earth's and upper mantle, Am. Geophy. Union, Washington, DC, 1969

[22] Zatopek A "Seismicity and related problems", Lecture note 9, Inter. Inst. Seism. Earthq. Engg., Tokyo, Japan, 1969

[23] Hattori S "Temporal variations of seismicity and seismic risk in and around Japan", Bull. Inter. Inst. Seism. Earthq. Engg., 17, 1978, 33-96

[24] Grunthal G "Earthquake Hazard" Lecture material, Vol. II, Seismology and hazard assessment, Potsdam, Germany, 1992

[25] Lee W H and Lahr J "A computer program for determining hypocenter, magnitude, and first motion pattern of local earthquakes", USGS Open File Report 75-311, 1975, 116p

[26] Karnik V "Seismicity of the European area", Geophy. Monogrph., The earth's crust and upper mantle, Am. Geophy. Union, Washington DC, 1969

[27] Miyamura S "Magnitude-frequency relation of earthquakes and its bearing in geotectonics", Proc. Japan Academy 38, 1962, 27-30

[28] Medvedev S V, Sponheuer W, and Karnik V " Intensity scale of earthquakes", IUGG, IASPEI, 7, Tagung, Europ. Seism. Kom, Vienna, 77.72, 1964

[29] Punsalan B T and Al-Amri A M "Scaling relations of earthquake parameters in the Red Sea regions", Jour. King Saud Univ. Sc (2), 15, 81-100

[30] Al-Amri A M "Seismicity of the south-western region of the Arabian Shield and southern Red Sea", Jour. Afr. Sc., 19(1/2, 17-25, 1994

[31] Al-Amri A M, Punsalan B T, and Uy E A "Seismic expectancy modeling of NW Saudi Arabia", Jour. Europ. Earthq. Engg., 1998

[32] Al-Amri A M, Punsalan B T, and Uy E A "Spatial distribution of the seismicity parameters in the Red Sea regions", Jour. Asian Sc. ,1998, 557-563

[33] Mogi K "Magnitude-frequency relation for elastic shocks accompanying fractures of various materials and some related problems in earthquakes", Bull. Earthq. Res. Inst., 40, 1962,831

[34] Wyss M "Towards a physical understanding of the earthquake frequency distribution", Geophy. Jour. Astr. Soc., 31, 1973, 341-359

[35] Scholz C "Microfractures, aftershocks and seismicity", Bull. Seism. Soc.Am., 58, 1968, 1117-1130

[36] Trifunac M D and Brady A G "On the correlation of seismic intensity scales with the peaks of recorded strong ground motion", Bull. Seism. Soc. Am., 65, 1965, 139-162

[37] Egloff F, Rihm R, Makris J, Izzeldin M, Bobsien D, Meier P, Junge T, Noman T, and Warsi W "Contrasting structural styles of the eastern and western margins of the southern Red Sea", Tectonophysics, 198, 1991, 329-353

[38] Richter H, Makris J, and Rihm R "Geophysical observation offshore Sdaudi Arabia: seismic and magnetic measurements", Tectonophysics, 198, 1991, 297-310

[39] El-Isa Z and Al-Shanti A "Seismicity and tectonics of the Red Sea and western Saudi Arabia", Geophy. Jour. Astr. Soc., 97, 1989, 449-457

[40] Schenk V "Seismic hazard assessment ", Lecture material, Vol. II, seismology and seismic hazard assessment, Potsdam, Germany, 1992

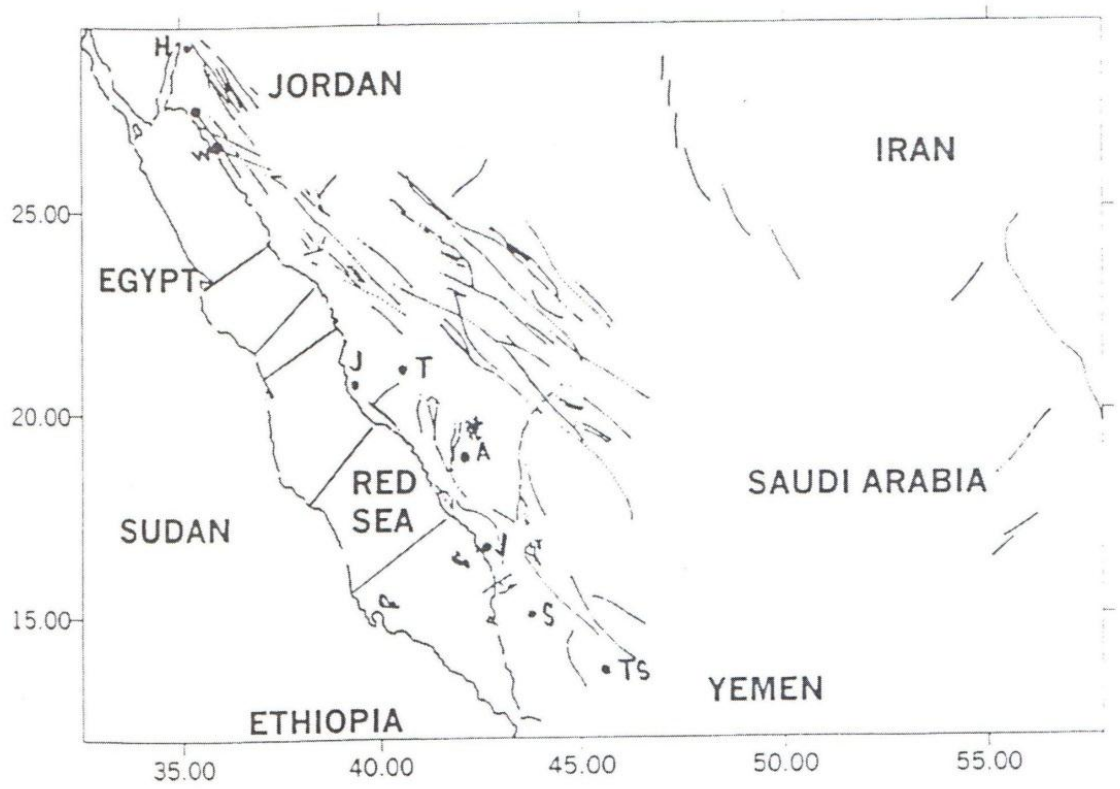

Fig. 1 : Tectonic and location map of the study area showing the geological structures and faults in Saudi Arabian peninsula and the Red Sea region as inferred from various sources.

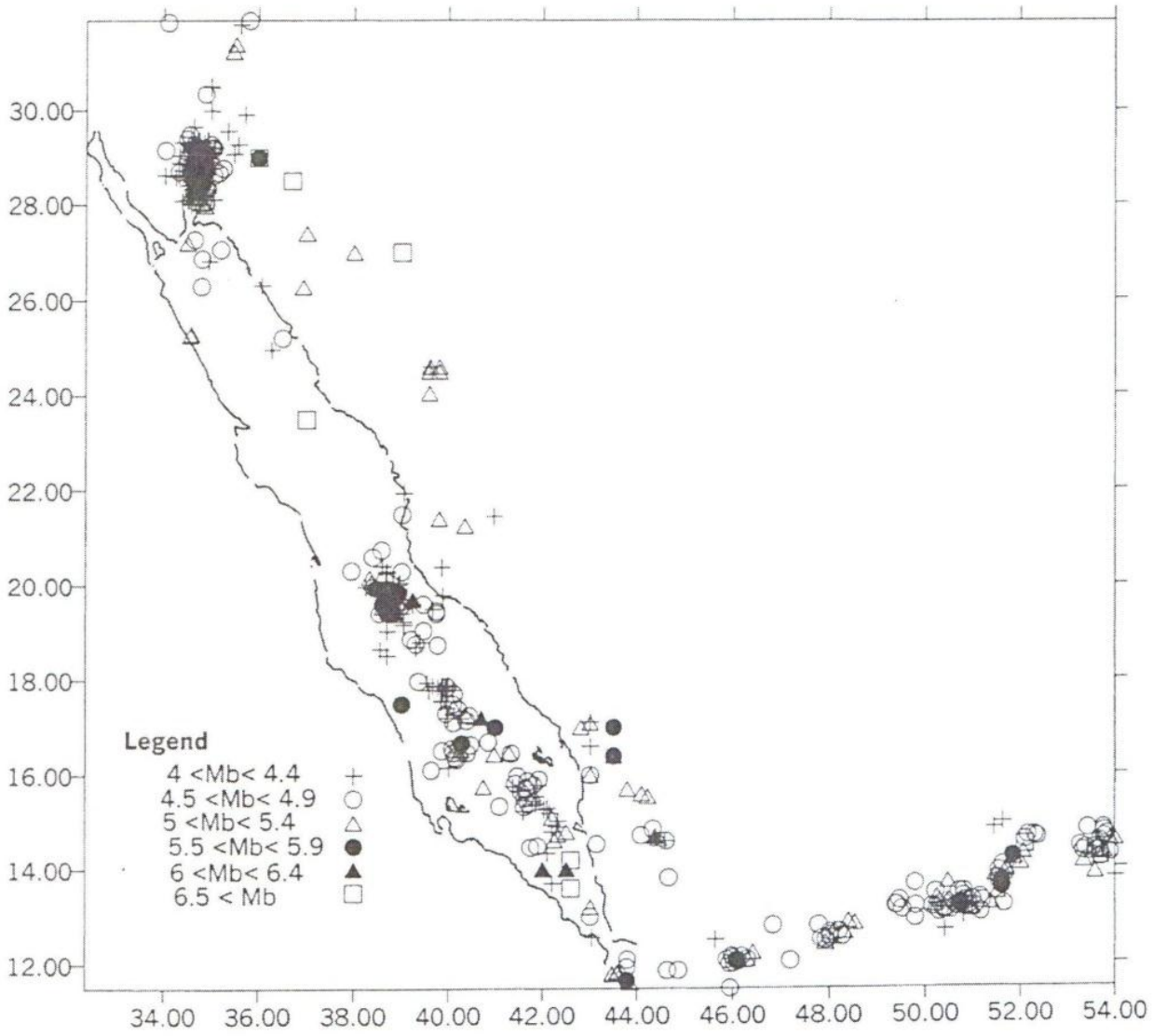

Fig. 2 : Spatial distribution of seismic events in Saudi Arabia and the Red Sea region as inferred from the merged various sources.

Fig. 3: Intensity attenuation equation utilized in seismic hazard assessment of western Saudi Arabia and the Red Sea region.

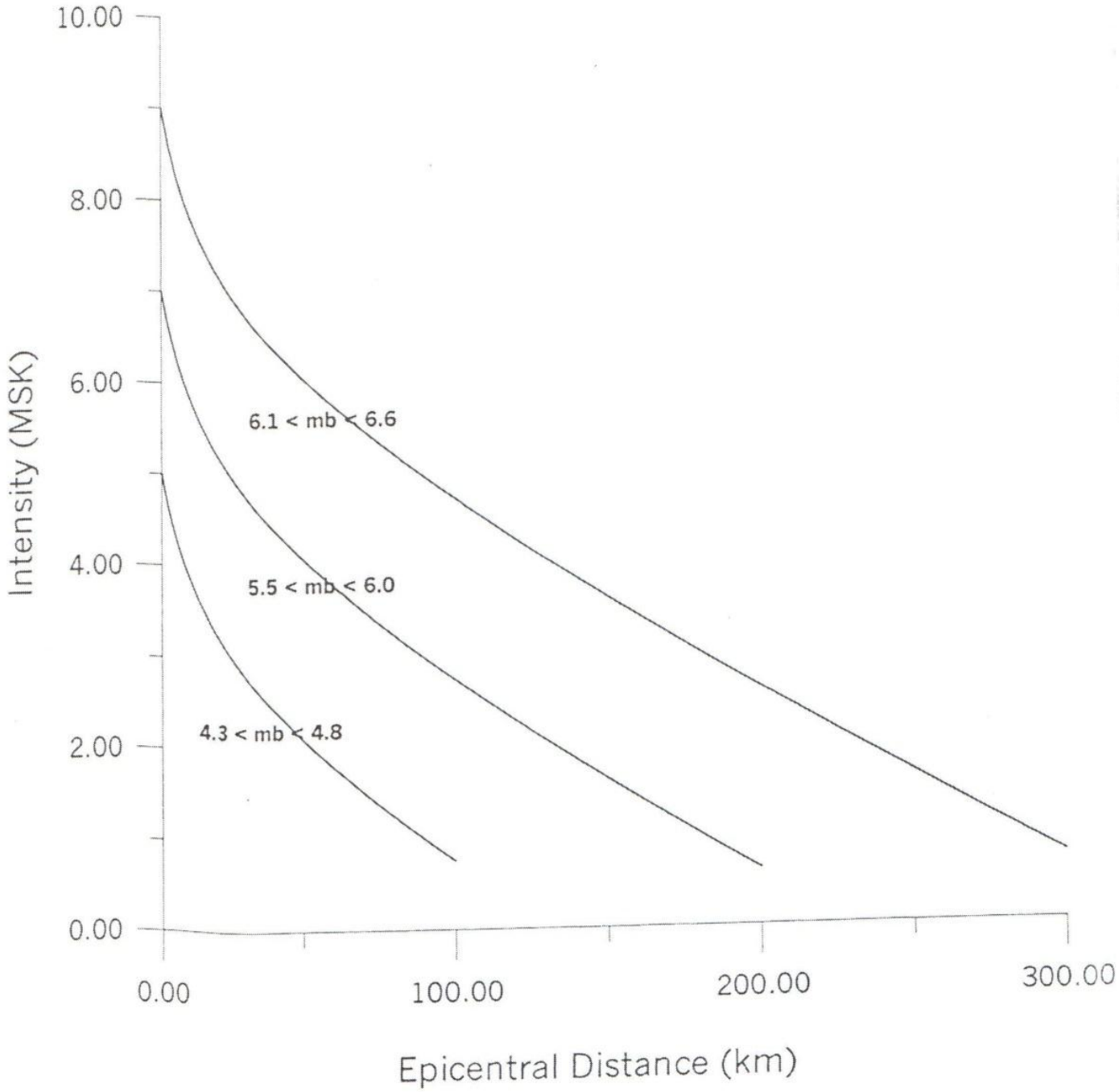

Fig. 4: Plot of surface-wave magnitude and intensity at the epicenter (solid circles). Line shows estimated linear relation.

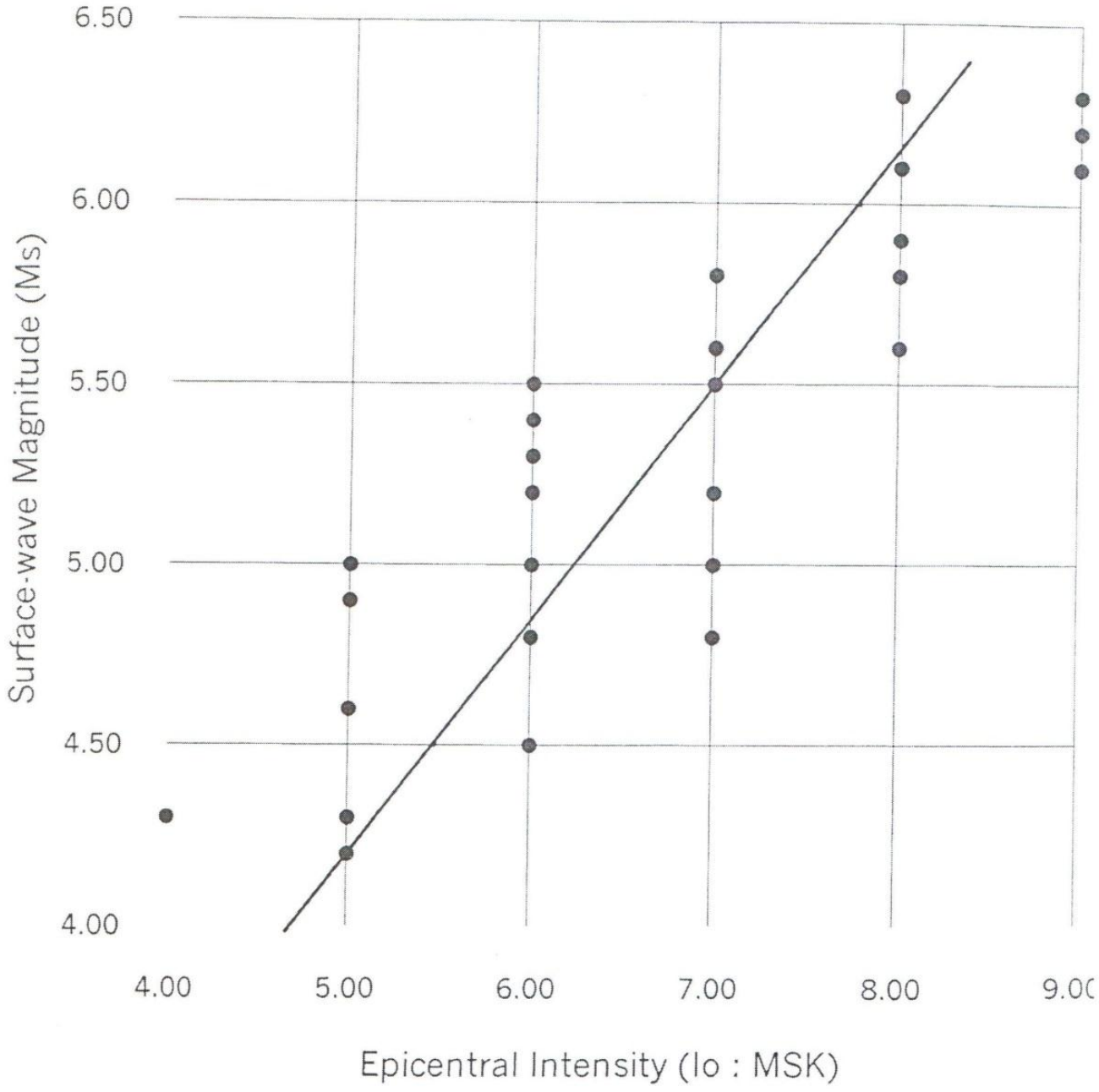

Fig. 5: Plot of frequency and intensity at the site 29.5N, 34.5E. Graph indicating an approximate logarithmic trend.

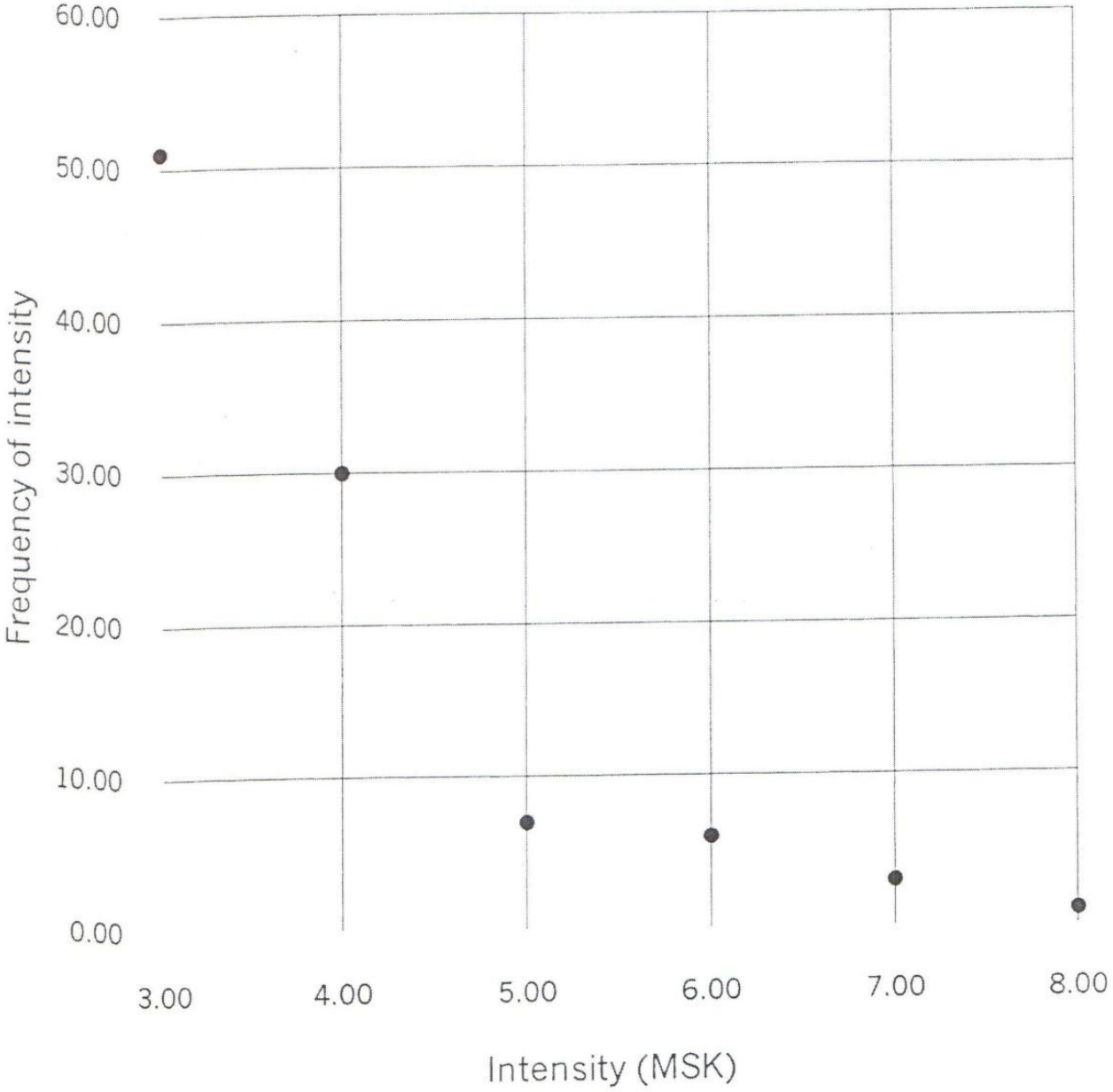

Fig. 6: Plot of the logarithm of the cumulative frequency and intensity at site 19N, 39E.

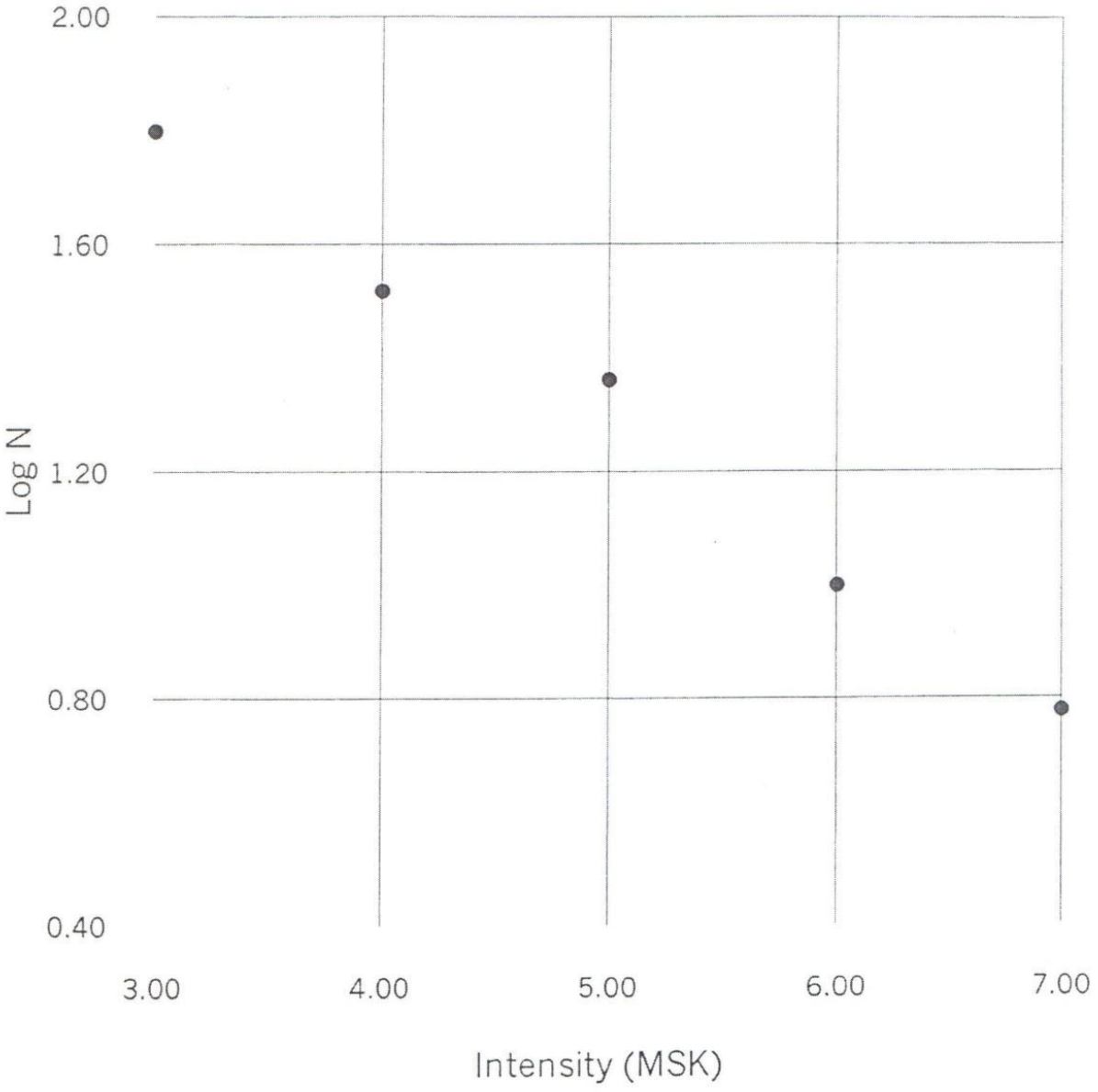

Fig. 7: Plot of the logarithm of the cumulative frequency and intensity at site 25N, 36E.

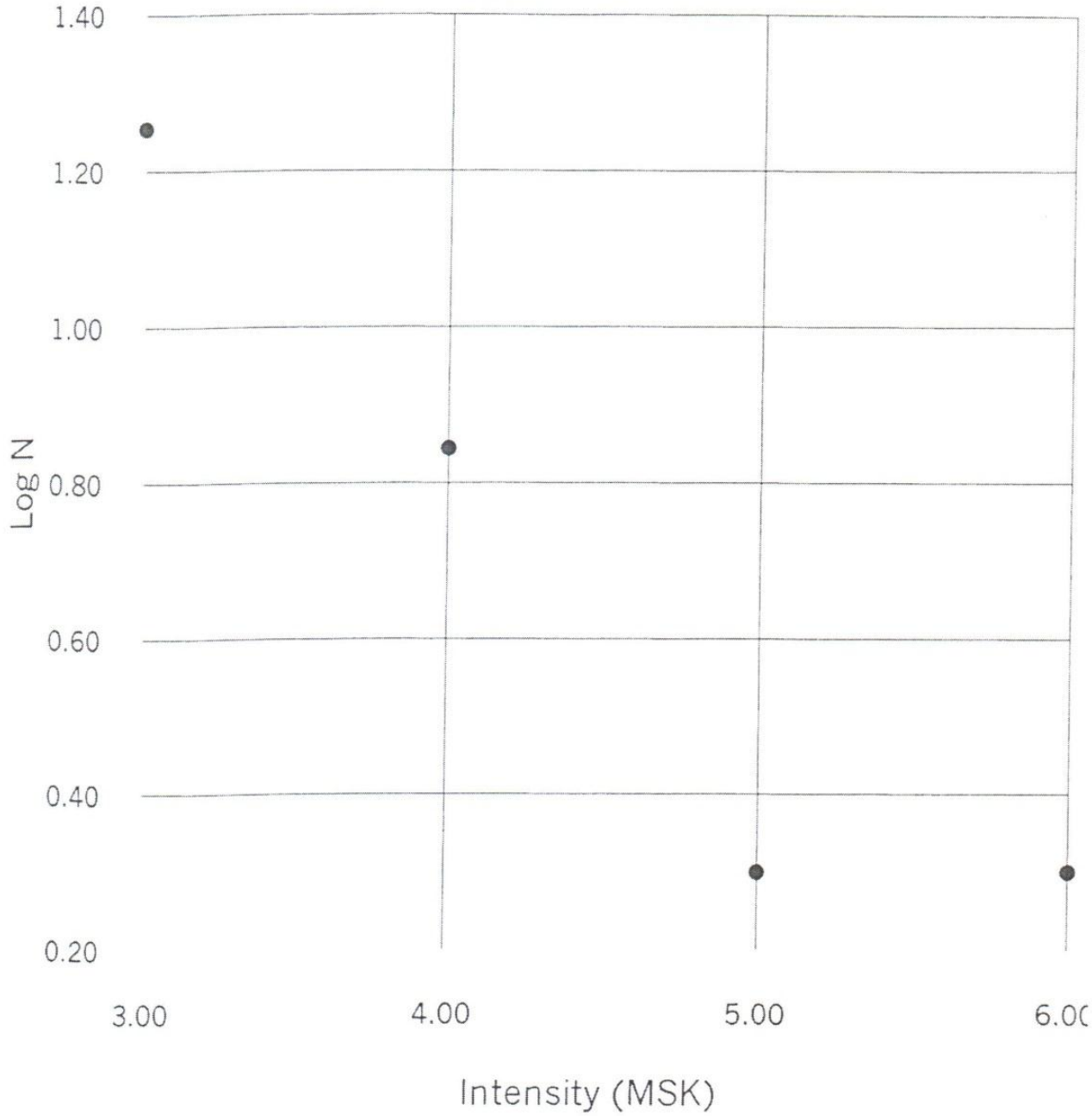

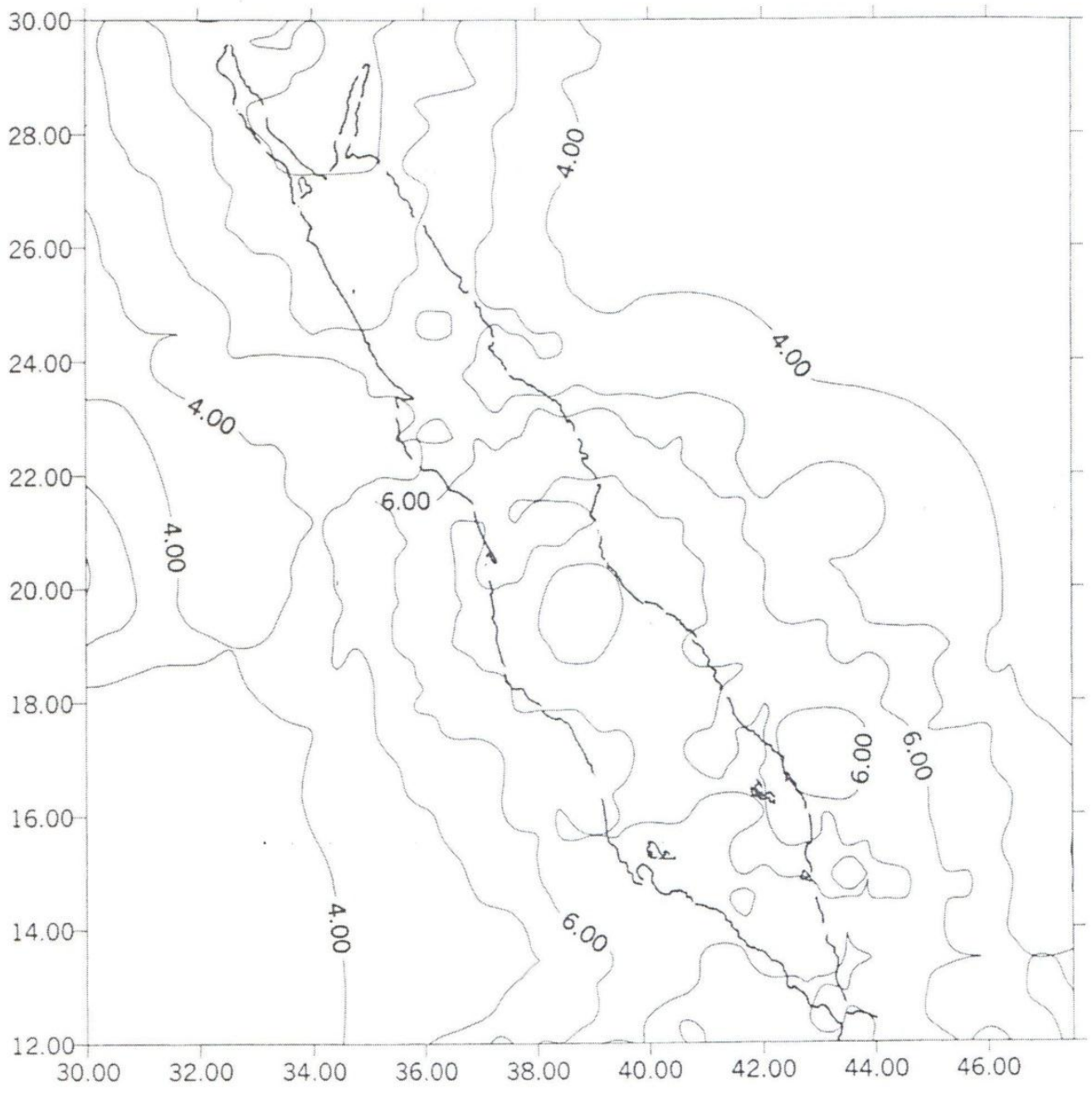

Fig. 8: Iso-intensity map of the expected maximum intensity (MSK) in 100 years at 10% probability of exceedance in western Saudi Arabia and the Red Sea region.

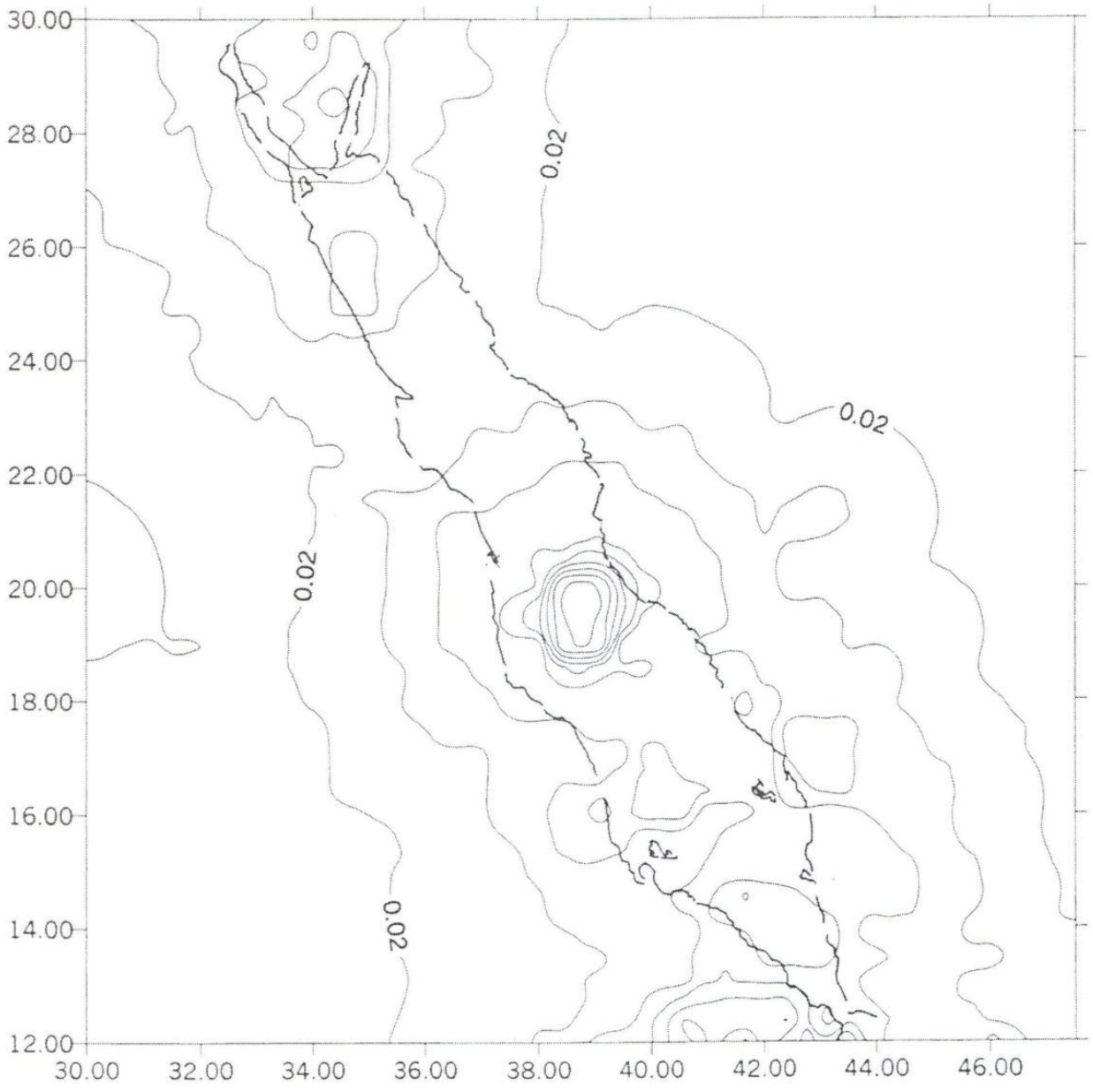

Fig. 9: Equivalent iso-acceleration map in percent of gravity (g) of the converted expected maximum intensity in western Saudi Arabia and the Red Sea region. Countours are: 0.02,0.05,0.1,0.15,0.2 0.25, 0.3, 0.35, and 0.4 of g.